Manifestation of quantum chaos in the spectra of quasi-one-dimensional surface superlattices

1998 J. Phys.: Condens. Matter 10 4001

(http://iopscience.iop.org/0953-8984/10/18/010)

J. Phys.: Condens. Matter **10** (1998) 4001–4014. Printed in the UK PII: S0953-8984(98)90592-6

Manifestation of quantum chaos in the spectra of quasi-one-dimensional surface superlattices

Hongqi Xu

Solid State Physics, Lund University, Box 118, S-221 00 Lund, Sweden

Received 12 January 1998

Abstract. Two statistical properties, namely, the energy level spacing distribution and the Dyson–Mehta Δ_3 statistics, are reported for the energy band structure of a confined, surface superlattice in perpendicularly applied magnetic fields. Time-reversal (T) symmetry is broken in the system. However, the system is invariant under the anti-unitary combination of symmetric operations which includes T, leading to what is called *false* time-reversal violation. For the wave vector k not in close vicinity of the symmetrical points in k-space, the statistical properties of the band structure at sufficiently strong magnetic fields are found to be described by Gaussian orthogonal ensemble (GOE) statistics. This result is a clear manifestation of quantum chaos in the system and is in agreement with the prediction that the false time-reversal violation suffices to give the energy spectra the properties of the GOE, instead of the Gaussian unitary ensemble. The spectra are found to deviate from the GOE statistics when the wave vector k is moved towards the symmetrical points in k-space and/or the magnetic field towards $B = 0$. This is because in these limit cases, the system is invariant under at least one geometric, symmetrical operation and hence spectral degeneracy becomes possible. The implications of this work for experiments are also discussed.

The idea of studying classically chaotic systems by analysis of the statistical properties of their quantum-mechanical energy spectra goes back to the fifties when Wigner proposed a new kind of statistical mechanics for the energy spectra of complex systems [1]. It is now well known that the statistical properties of the energy spectra are universal [2–4]: they depend only on the symmetries of the Hamiltonian and not on the details of the dynamic properties of the systems. Thus, the distribution of n consecutive energy levels of a given system is statistically equivalent to the behaviour of n consecutive eigenvalues chosen from an ensemble of random matrices with a corresponding symmetry.

Using the language of random-matrix theory (RMT), three symmetry classes of random-matrix ensembles are defined to describe the statistical properties of correlated energy levels: systems in which the time-reversal symmetry is broken are described by the unitary ensemble; time-reversal-invariant systems are described by either the orthogonal or the symplectic ensemble depending on whether or not the systems are, in addition, invariant under rotation. Uncorrelated energy levels are, however, described by the Poisson statistics.

In this paper, we report a statistical analysis of the energy spectra of a confined, two-dimensional (2D), antidot superlattice in perpendicularly applied magnetic fields. The work is motivated by recent experimental [5] and theoretical [6] studies of electron transport in similar systems, namely, finite antidot lattices. It was observed that the conductance of these systems exhibits strong, irregular oscillations whose detail is very sensitive to the

0953-8984/98/184001+14$19.50

potential profile of the systems. Since the peaks in the oscillations can be associated with the transmission through electron states [6], this irregularity manifests that the systems have complicated, system-dependent electronic spectra. One is then led to ask whether there is some universal (system-independent) behaviour in the apparently very complicated spectra. In a preliminary study [7], an indication of the universality was observed in a periodic superlattice of this type. The present paper will be devoted to a detailed study and discussion of the universal behaviour in the energy spectra of the system.

For an infinite, 2D, antidot superlattice, it was found [8, 9] that the statistical behaviour of the magnetic band structure depends strongly on the magnetic wave vector and on the number of magnetic flux quanta penetrating a unit cell. For a rational number of flux quanta, the magnetic band structure does not show the statistical features of chaos when the flux denominator is sufficiently large [8]. For an integer number of flux quanta, the energy levels at a non-symmetric point in the magnetic wave-vector space are described by the Gaussian unitary ensemble (GUE) statistics, while the Gaussian orthogonal ensemble (GOE) or (almost) Poisson statistics are found in the magnetic band structure at a symmetric point [8]. However, the GUE statistics was not found at all, in the preliminary study of reference [7], in the magnetic band structure of a confined, 2D, antidot superlattice where time-reversal (T) symmetry is broken. Instead, the band structure of the system was found to possess the properties of the GOE in a large range of magnetic fields. The reason for this will be explained in more detail in this work.

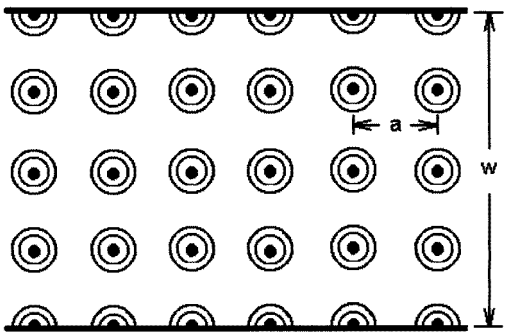

Figure 1. A schematic view of the square, antidot superlattice confined in a square-well quantum channel with hard walls. In this work, the lattice potential was modelled by a smooth function given in equation (1). The period of the lattice and the width of the channel were taken to be $a = 100$ nm and $w = 400$ nm, respectively. As a result, the superlattice has four periods across the channel.

The system that we have considered is a square, antidot lattice implanted in the x–y plane with a period a in a wide channel of width w as shown in figure 1. The potential of the antidot lattice will be described by a realistic model of the form

$$V(x, y) = V_0 \{\cos[\pi x/a] \cos[\pi y/a]\}^{2\beta} \tag{1}$$

where $|x| < \infty$ and $|y| \leqslant w/2$, while V_0 and integral β control the strength and steepness of the antidot potential. This type of potential was used by Fleischmann, Geisel and Ketzmerick [10] in the study of classical electron dynamics in a free, 2D, antidot superlattice. In the present work, the assumption that $V_0 = 1$ eV and $\beta = 10$ was made for the periodic antidot potential, and a square-well potential with hard walls was used to define the channel. The lattice spacing was taken to be $a = 100$ nm and the width of the square well $w = 400$ nm,

so that the antidot potential has four periods along the y-direction (figure 1). The motion of a spinless electron in the system inside the channel is described by the Hamiltonian

$$H = \frac{1}{2m^*}[\boldsymbol{P} + e\boldsymbol{A}(x, y)]^2 + V(x, y) \tag{2}$$

where m^* is the electron effective mass, and $\boldsymbol{A} = (-By, 0, 0)$ is the vector potential in the Landau gauge. The assumption was made in this work that the mass $m^* = 0.067m_e$, which is appropriate for an $Al_xGa_{1-x}As$/GaAs 2D electron system. In equation (2), the magnetic field $\boldsymbol{B} = (0, 0, B)$ breaks time-reversal symmetry. Furthermore, with the potential defined in equation (1), the system is, in general, classically not integrable and the classical dynamics in the system is very likely to be chaotic. We therefore expect the quantum-mechanical energy spectra of the system to show the signature of quantum chaos, namely, spectral correlations.

The translation invariance of the Hamiltonian allows us to reduce the quantum-mechanical problem to the study of the electron motion in a single unit cell. Using Bloch's theorem, the Schrödinger equation can be written as

$$H_k u_k(x, y) = E(k)u_k(x, y) \tag{3}$$

where k is the Bloch momentum, or the wave vector, in the x-direction, $u_k(x + a, y) = u_k(x, y)$ is the periodic part of the single-electron wave function and the reduced Hamiltonian is

$$H_k = -\frac{\hbar^2}{2m^*}\left(\frac{\partial^2}{\partial x^2} + \frac{\partial^2}{\partial y^2}\right) - \frac{\mathrm{i}\hbar^2}{m^*}\left(k - \frac{eBy}{\hbar}\right)\frac{\partial}{\partial x} + \frac{\hbar^2}{2m^*}\left(k - \frac{eBy}{\hbar}\right)^2 + V(x, y). \tag{4}$$

Equation (3) with the Hamiltonian given in equation (4) was solved numerically for a given wave vector k and magnetic field B on the basis of functions of the form

$$\Phi_{\ell m}(x, y) = \frac{1}{a^{1/2}} \exp(\mathrm{i}K_\ell x)\phi_m(y) \tag{5}$$

where $K_\ell = 2\pi\ell/a$ with $\ell = 0, \pm1, \pm2, \ldots, \pm\infty$ and $\phi_m(y)$ with $m = 1, 2, \ldots, \infty$ are the transverse eigenfunctions of the pure quantum channel. The magnetic band structure of the system was obtained by presenting the calculated eigenvalues $E_n(k)$ (with n being the band index) as a function of the wave vector k for each magnetic field value B. Because the band structure is symmetric with respect to $k = 0$, only the half of the band structure for the wave vector in the range $0 \leqslant k \leqslant \pi/a$ was actually calculated and used for the spectral statistics.

The typical magnetic band structure of the system is presented in figure 2, where the energy band correlations can be seen. It is shown that when the wave vector k is moved away from $k = 0$ and π/a, the energy bands may approach each other, but will never cross. The energy bands always tend to repel, when they come very close, and show anti-crossings. We notice that the energy band correlations were also observed in the electronic structure of the silicon crystal and the $Al_xGa_{1-x}As$ alloy by Mucciolo and co-workers [11].

As a result of this type of correlation, the statistical properties of the magnetic band structure are expected to be described by the statistics of a random-matrix ensemble. It can be easily verified that the reduced Hamiltonian H_k given in equation (4) is, in general, invariant neither under T nor under any geometric symmetrical operation—for example, the reflection R_x $(x \to -x)$. However, the Hamiltonian is invariant under the anti-unitary operation TR_x; that is, it possesses a *false* time-reversal violation. It has been shown [12] that this false T-violation is sufficient to lead to GOE statistics, rather than GUE statistics as one might naively have assumed.

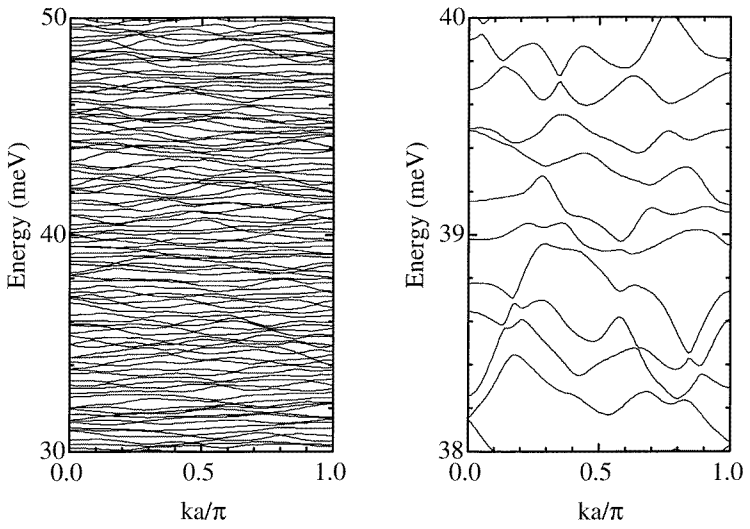

Figure 2. Typical magnetic band structure of the confined, surface superlattice as shown in figure 1. The left-hand panel shows the band structure calculated at an applied magnetic field $B = 0.5$ T for about 100 energy bands, corresponding to the band index $n \approx 150$ to 250. The right-hand panel is a portion of the band structure plotted on an expanded energy scale. Notice the anti-crossings of the energy bands at $k \neq 0$ and π/a.

The two most frequently studied characteristics of spectral statistics are the level spacing distribution $P(s)$, where s is the nearest-neighbour band spacing (hereafter we will always express energies in units of the mean band spacing and refer to $P(s)$ as the band spacing distribution), and the Dyson–Mehta statistics Δ_3 [13]. $P(s)$ measures the band repulsion; it is normalized. Δ_3 measures the rigidity of the spectrum; it is given by the variance of the number of energy eigenvalues found in an energy interval of length L:

$$\Delta_3(L) = \frac{1}{L}\left\langle \min_{a,b} \int_{\bar{E}-L/2}^{\bar{E}+L/2} \mathrm{d}E\ [N(E) - aE - b]^2 \right\rangle \tag{6}$$

where $N(E)$ is the number of energy levels below the energy E and the angle brackets indicate the statistical average which we will specify later.

In terms of RMT, $P(s)$ and Δ_3 can be approached using analytical expressions [2]. For a correlated energy band sequence, one has

$$P(s) = N_\beta s^\beta \exp(-C_\beta s^2) \tag{7}$$

where $\beta = 1$, $C_1 = \pi/4$ and $N_1 = \pi/2$ for the GOE, and $\beta = 2$, $C_2 = 4/\pi$ and $N_2 = 32/\pi^2$ for the GUE. The Dyson–Mehta statistics for a correlated energy band sequence is [2]

$$\Delta_3(L) = \frac{1}{15}L^{-4}\left[L^5 - \int_0^L \mathrm{d}u\ (L-u)^3(2L^2 - 9Lu - 3u^2)Y_\beta(u)\right] \tag{8}$$

where $Y_\beta(u)$ is the two-level cluster function given by

$$Y_1(u) = \left[\frac{\sin(\pi u)}{\pi u}\right]^2 + \frac{\mathrm{d}}{\mathrm{d}u}\left[\frac{\sin(\pi u)}{\pi u}\right]\int_u^\infty \mathrm{d}t\ \frac{\sin(\pi t)}{\pi t} \qquad \text{for } \beta = 1 \text{ (GOE)} \tag{9}$$

$$Y_2(u) = \left[\frac{\sin(\pi u)}{\pi u}\right]^2 \qquad \text{for } \beta = 2 \text{ (GUE).} \tag{10}$$

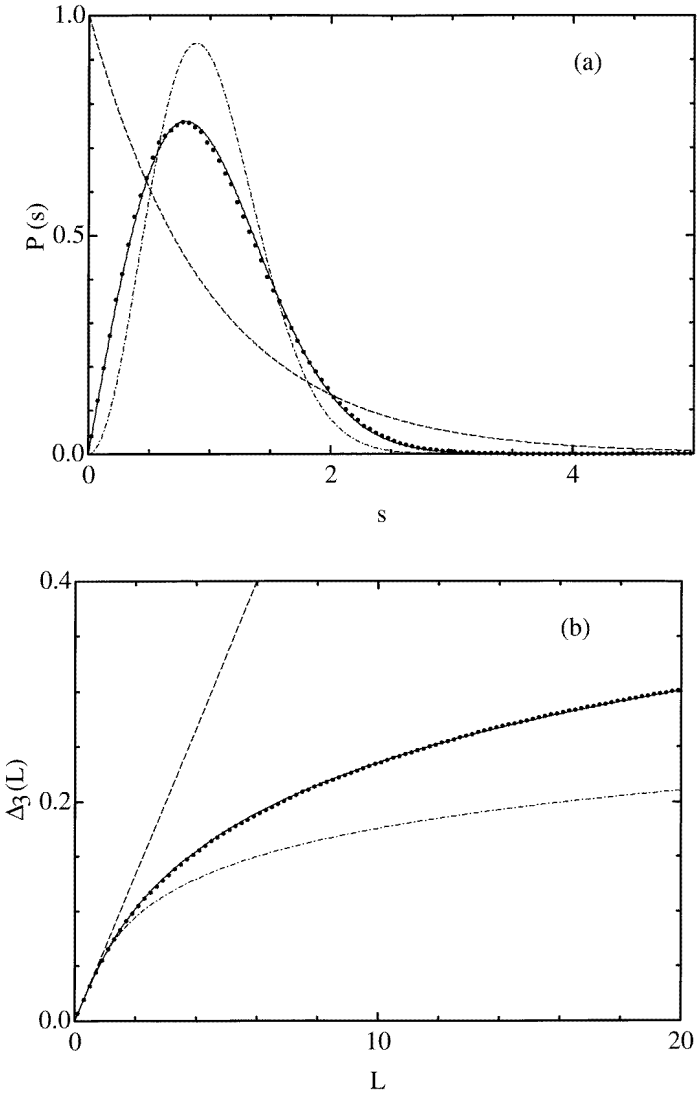

Figure 3. The spectral statistics for the magnetic band structure of the confined, surface superlattice as shown in figure 1. The data were extracted from the energy eigenvalues of 301 energy bands with the band index $n = 200$ to 500, 41 equally spaced k-points in the range $k = 0.3\pi/a$ to $0.7\pi/a$ and 71 equally spaced magnetic field values in the range $B = 0.3$ to 1 T. (a) shows the band spacing distribution $P(s)$; (b) shows the Dyson–Mehta statistics $\Delta_3(L)$. The full, chain, and dashed curves give the theoretical predictions for the GOE, GUE and Poisson statistics, respectively.

When the bands are completely uncorrelated, one has Poisson statistics of $P(s) = \mathrm{e}^{-s}$ and $\Delta_3(L) = L/15$ [2].

The numerical calculations of these two statistical characteristics for our system proceeded as follows. We first generated a number of magnetic band structures for the system by shifting the magnetic field by steps of 0.01 T. In each magnetic energy band structure, the energy eigenvalues for a finite number of k-points with an equal spacing of

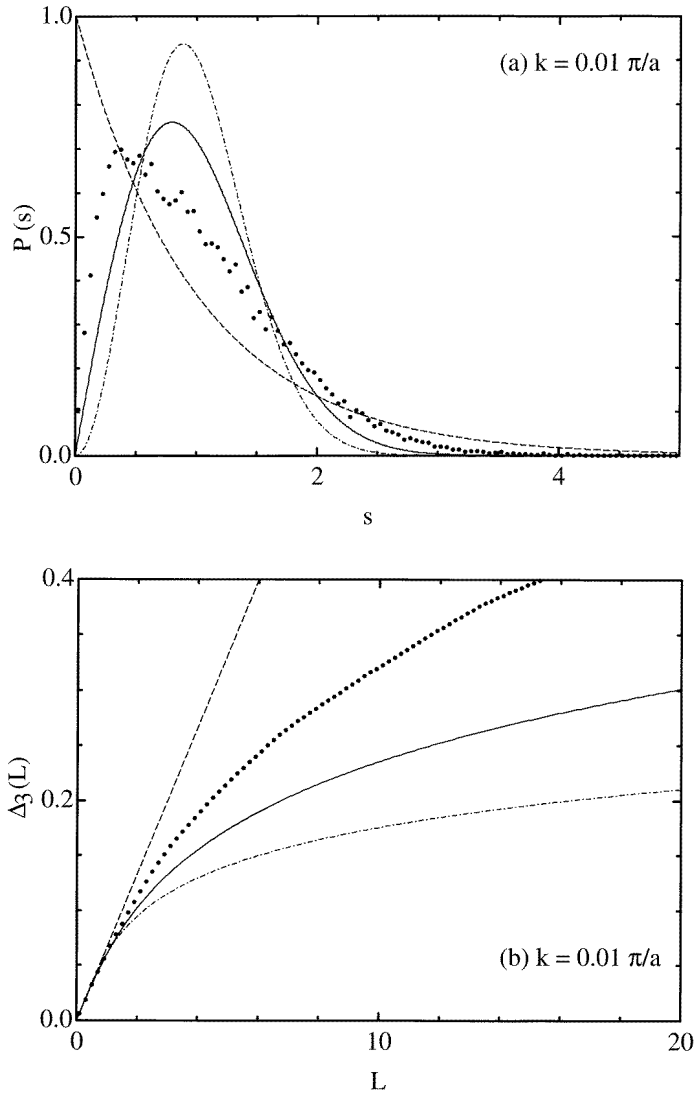

Figure 4. The spectral statistics for the magnetic band structure of the confined, surface superlattice as shown in figure 1 at different k-values. The data for each k-value were extracted from the energy eigenvalues of 501 energy bands with the band index $n = 100$ to 600 and 71 equally spaced magnetic field values in the range $B = 0.3$ to 1 T. (a) and (b) show the band spacing distribution $P(s)$ and the Dyson–Mehta statistics $\Delta_3(L)$, respectively, for $k = 0.01\pi/a$; (c) and (d) those for $k = 0.04\pi/a$; (e) and (f) those for $k = 0.07\pi/a$; (g) and (h) those for $k = 0.10\pi/a$. The full, chain, and dashed curves give the theoretical predictions for the GOE, GUE and Poisson statistics, respectively.

$\Delta k = 0.01\pi/a$ were considered. The statistical average was taken over different values of the magnetic field and the wave vector k, and over a large number of energy bands. (Note that in the calculations for the Δ_3 statistics, the average over the energy bands was taken over those values of $\bar{E}$ for which the intervals defined between $\bar{E} - L/2$ and $\bar{E} + L/2$ do not overlap.) The energy values at $k = 0$ and π/a were excluded from the statistical average,

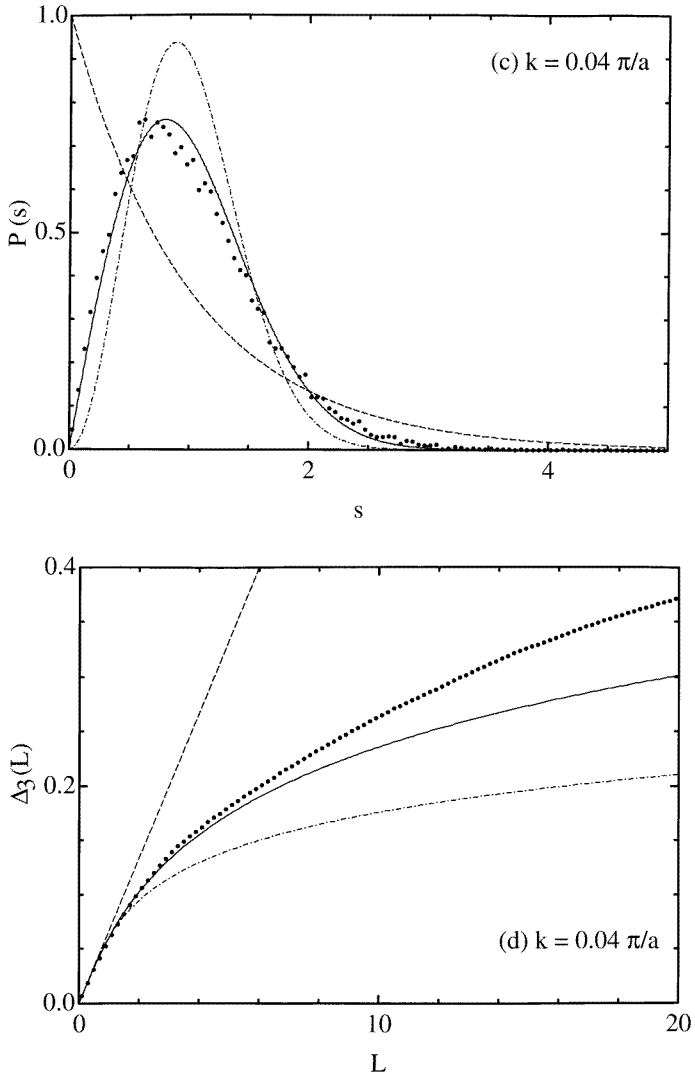

Figure 4. (Continued)

because in this case H_k is invariant under space inversion and the occurrence of degeneracy is thus possible.

The spectra need to be unfolded before being statistically averaged. There are different ways of unfolding the spectra [14, 15]. In this work, the spectral unfolding was carried out in the following way. Let us explicitly write the energy band eigenvalues, before expressing them in units of the mean band spacing, as $E_n(k_i, B_j)$ ($n = 0, 1, \ldots, N$; $i = 1, \ldots, K$; $j = 1, \ldots, M$). The spacings between adjacent energy levels are

$$S_n^{(i,j)} = E_n(k_i, B_j) - E_{n-1}(k_i, B_j) \qquad n = 1, \ldots, N. \tag{11}$$

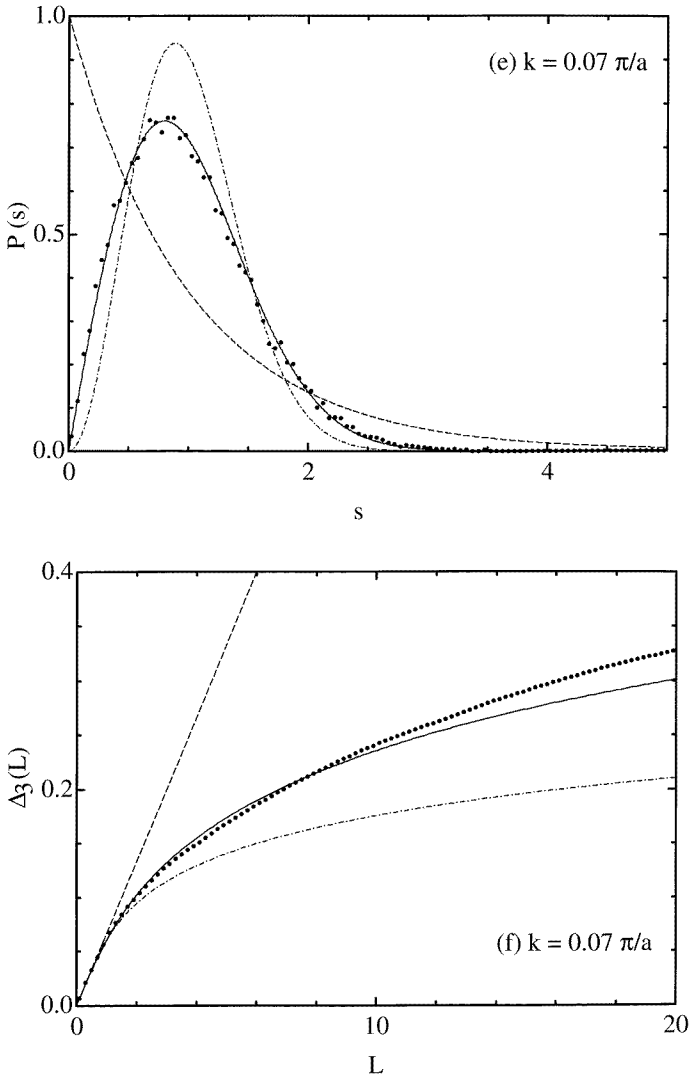

Figure 4. (Continued)

The set $\{S_n^{(i,j)}\}$ has then been replaced by the set $\{s_n^{(i,j)}\}$ where

$$s_n^{(i,j)} = \frac{S_n^{(i,j)}}{\overline{S_n}} \tag{12}$$

with

$$\overline{S_n} = \frac{1}{KM} \sum_{i=1}^{K} \sum_{j=1}^{M} S_n^{(i,j)}. \tag{13}$$

Now the spectra corresponding to the set $\{s_n^{(i,j)}\}$ are unfolded in the sense that the level

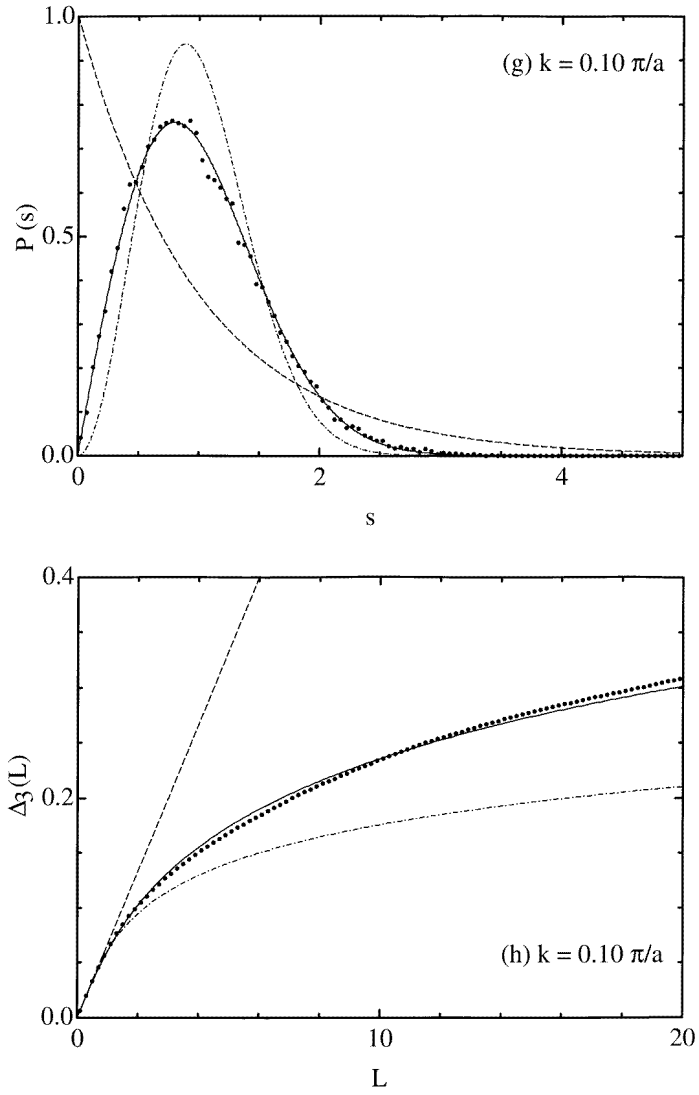

Figure 4. (Continued)

density in the spectra is statistically uniform, i.e.,

$$\overline{s_n} = \frac{1}{KM}\sum_{i=1}^{K}\sum_{j=1}^{M} s_n^{(i,j)} = 1 \qquad \text{for all } n. \tag{14}$$

The unfolded spectra were then expressed in units of the mean energy band spacing which was evaluated at each pair of given values of k and B.

The results of our calculations of the statistical properties of the energy spectra of the surface superlattice are summarized in figures 3–5. In these figures the comparison of our results with the RMT predictions are also presented. Figure 3 shows our numerical results extracted from a set of the energy eigenvalues in the magnetic energy bands with band index $n = 200$ to 500 (corresponding to the energy range between about 40 and 100 meV)

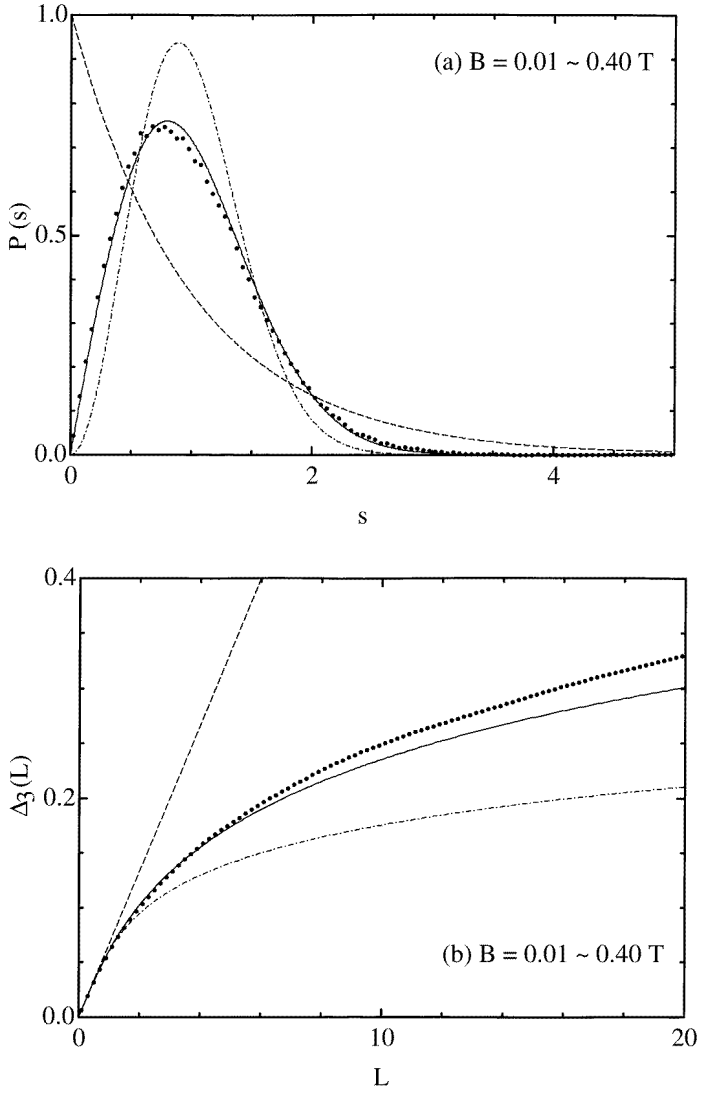

Figure 5. The spectral statistics for the magnetic band structure of the confined, surface superlattice as shown in figure 1 in three different ranges of the magnetic field. The data for each range of magnetic field were extracted from the energy eigenvalues of 101 energy bands with the band index $n = 300$ to 400, 61 equally spaced k-points in the range $k = 0.2\pi/a$ to $0.8\pi/a$ and 40 equally spaced magnetic field values. (a) and (b) show the band spacing distribution $P(s)$ and the Dyson–Mehta statistics $\Delta_3(L)$, respectively, for $B = 0.01$ to 0.40 T; (c) and (d) those for $B = 0.11$ to 0.50 T; (e) and (f) those for $B = 0.21$ to 0.60 T. The full, chain and dashed curves give the theoretical predictions for the GOE, GUE and Poisson statistics, respectively.

computed for 41 k-points and 71 magnetic field values. These k-points (equally spaced in the range $0.3\pi/a$ to $0.7\pi/a$) and magnetic field values (equally spaced in the range 0.3 to 1 T) are chosen such that the correlations between the energy bands are well developed. Notice the good agreement with the RMT predictions for the GOE. This is in contrast to

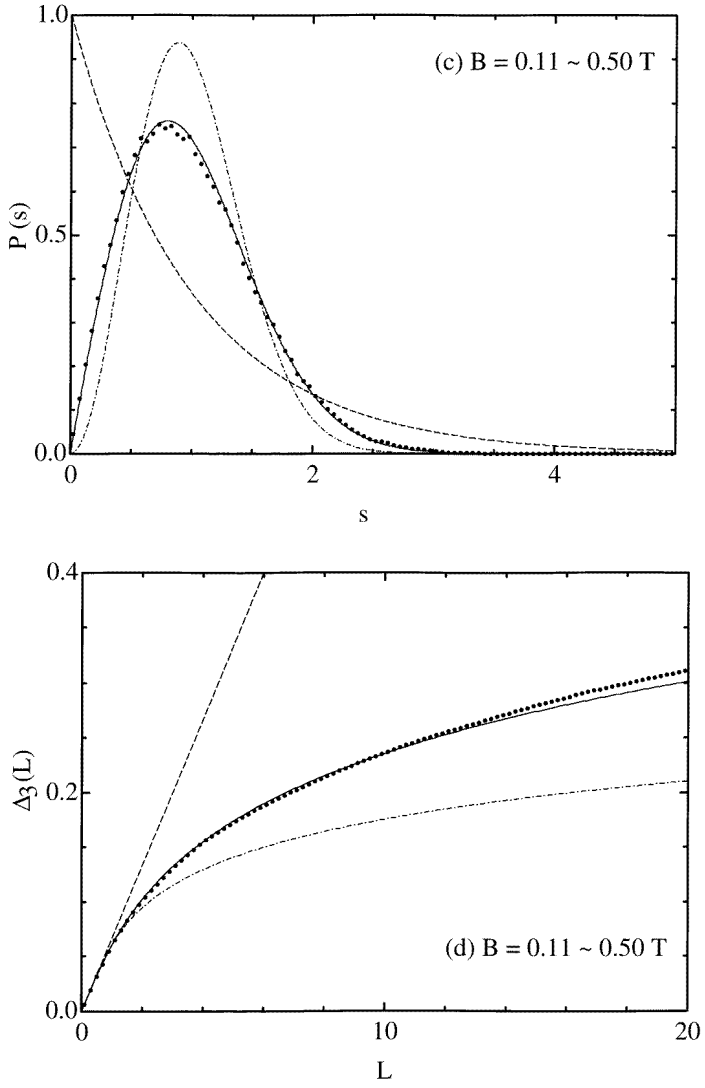

Figure 5. (Continued)

the work of references [8, 9] on the magnetic band structure of a 2D, surface superlattice where GUE statistics, instead of GOE statistics, was reported for the energy spectra at non-symmetric points in the magnetic wave-vector space. However, our results are consistent with the prediction [12] that although time-reversal symmetry and all geometric symmetries are broken in the Hamiltonian H_k (equation (4)) of the system, the symmetry under the anti-unitary combination TR_x should lead to the statistics of the GOE.

As we pointed out, the Hamiltonian H_k given in equation (4) is invariant under the space inversion (P) at $k = 0$ or π/a, the space reflection $y \to -y$ (R_y) at $B = 0$, or R_x, R_y, and P at $k = 0$ and $B = 0$ or $k = \pi/a$ and $B = 0$. Deviations from GOE statistics are therefore expected in the statistical properties of the energy spectra when k approaches zero or π/a, and/or B approaches zero. This is demonstrated in figures 4 and 5.

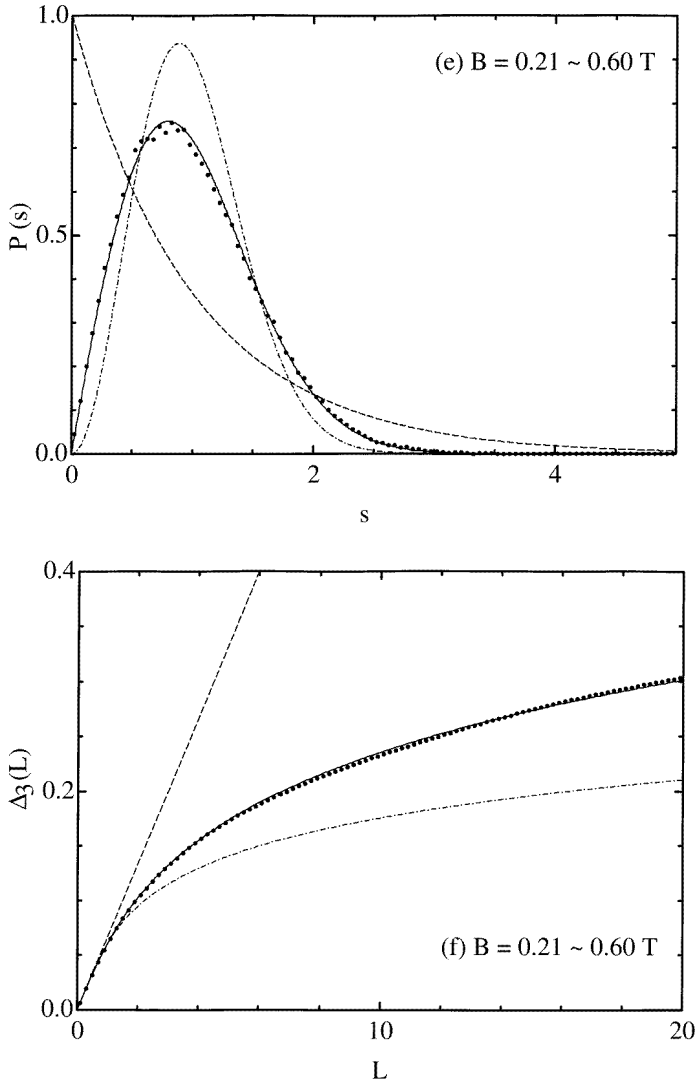

Figure 5. (Continued)

Figure 4 shows the band spacing distribution $P(s)$ and the Δ_3 statistics extracted from the energy eigenvalues of about 500 energy bands ($n = 100$–600) and 70 equally spaced magnetic field values in the range $B = 0.3$ to 1 T at four individual wave vectors, namely, $k = 0.01\pi/a, 0.04\pi/a, 0.07\pi/a$ and $0.1\pi/a$. A clear deviation from GOE statistics is seen as we move the wave vector k towards $k = 0$. The same result was also found as we move the wave vector towards $k = \pi/a$. This deviation can be simply understood as follows: in the limit cases of $k = 0$ or $k = \pi/a$, twofold spectral degeneracy is possible, because of the existence of the space inversion (P) symmetry in the Hamiltonian H_k (see equation (4)). Thus, the energy levels in the spectra can be divided into two categories according to the parity of their wave functions under P. In each category, the spectra show GOE statistics. The full spectra of the system show the statistics resulting from a

superposition of two independent spectra with GOE statistics. It was shown [16] that the level spacing distribution $P(s)$ for the superposed spectra has a non-zero value at $s = 0$. However, the spectral statistics presented in figure 4 shows that $P(s) = 0$ at $s = 0$. This difference results simply from the fact that the energy levels at $k = 0$ and $k = \pi/a$ have been explicitly excluded from the level statistics in this work.

In figure 5, we show the band spacing distribution $P(s)$ and the Δ_3 statistics of the energy spectra for three ranges of the magnetic field. The overlaps between these three ranges were allowed in order to create a sufficient number of data for the statistical average. The data in each magnetic field range were extracted from the energy eigenvalues in about 101 energy bands ($n = 300$ to 400), 61 equally spaced k-points ($k = 0.2\pi/a$ to $0.8\pi/a$), and 40 magnetic field values (with an equal spacing $\Delta B = 0.01$ T). The deviations from the RMT predictions for the GOE are clearly visible in the statistical properties of the energy spectra at low magnetic fields (figures 5(a) and 5(d)), while good agreement with the RMT predictions is seen in the statistical properties of the energy spectra at magnetic fields beyond $B = 0.2$ T (figures 5(e) and 5(f)). The result is seen more clearly in the Δ_3 statistics, but the indication is still visible in the band spacing distribution $P(s)$. The deviations seen in this figure can be understood in the same way as the above.

The statistical properties of the correlated spectra in the system should be observable experimentally. Methods suitable for the fabrication of such a confined, surface superlattice are available today (see, for example, references [5, 17, 18]). The energy states above the Fermi level can be detected by optical methods from either inter-band or intra-band transitions. A tunable magnetic field can be applied to the system in order to obtain a large number of data and hence facilitate the statistical analysis.

To summarize, we have reported a numerical study of the two statistical properties, namely, the energy band spacing distribution $P(s)$ and the Dyson–Mehta statistics $\Delta_3(L)$, for the magnetic band structure of a confined, surface superlattice in perpendicularly applied magnetic fields. The time-reversal symmetry is broken in the system due to the presence of the magnetic fields. However, the reduced Hamiltonian H_k given in equation (4) shows a false time-reversal violation, i.e., it is invariant under the anti-unitary combination TR_x. Since the magnetic band structure of the system is symmetric with respect to $k = 0$, only the half of the band structure for the wave vector in the range $0 \leqslant k \leqslant \pi/a$ has been considered in the spectral analysis. For the wave vector k not in the close vicinity of the symmetrical points of $k = 0$ and π/a, the magnetic band structures at sufficiently strong magnetic fields are found to exhibit GOE statistics, in agreement with the prediction that the false time-reversal violation is sufficient for the energy spectra to possess the properties of the GOE, instead of the GUE. The appearance of GOE or GUE statistics is usually associated with quantum chaos. The spectral statistics is found to deviate from GOE statistics when the wave vector k is moved close to $k = 0$ or π/a, and/or the magnetic field is moved close to $B = 0$, because in these limit cases, the Hamiltonian H_k is invariant under at least one geometric, symmetrical operation and hence the spectral degeneracy becomes possible. The implications of this work for experiments have also been discussed.

Acknowledgments

This work, which was carried out within the Nanometre Structure Consortium in Lund, has been supported by the Swedish Natural Science Research Council (NFR), the Swedish Research Council for Engineering Sciences (TFR), and the Swedish National Board for Industrial and Technical Development (NUTEK).

References

[1] Wigner E P 1951 *Proc. Camb. Phil. Soc.* **47** 790
Dyson F J 1962 *J. Math. Phys.* **3** 140
[2] Mehta M L 1991 *Random Matrices* (New York: Academic)
[3] Bohigas O 1991 *Chaos and Quantum Physics* ed M-J Giannoni, A Voros and J Zinn-Justin (Amsterdam: Elsevier)
[4] Haake F 1991 *Quantum Signatures of Chaos* (Berlin: Springer)
[5] Schuster R, Ensslin K, Wharam D, Kühn S, Kotthaus J P, Böhm G, Klein W, Tränkle G and Weimann G 1994 *Phys. Rev.* B **49** 8510
[6] Xu Hongqi 1994 *Phys. Rev.* B **50** 12 254
[7] Xu Hongqi 1996 *Proc. 23rd Int. Conf. on the Physics of Semiconductors* vol 2, ed M Scheffler and R Zimmermann (Singapore: World Scientific) p 1489
[8] Silberbauer H, Rotter P, Rössler U and Suhrke M 1995 *Europhys. Lett.* **31** 393
[9] Steffens O, Suhrke M and Rotter P 1997 *Phys. Rev.* B **55** 4486
[10] Fleischmann R, Geisel T and Ketzmerick R 1992 *Phys. Rev. Lett.* **68** 1367
[11] Mucciolo E R, Capaz R B, Altshuler B L and Joannopoulos J D 1994 *Phys. Rev.* B **50** 8245
[12] Robnik M and Berry M V 1986 *J. Phys. A: Math. Gen.* **19** 669
[13] Bohigas O, Giannoni J M and Schmit C 1984 *Phys. Rev. Lett.* **52** 1
Bohigas O and Giannoni J M 1984 *Mathematical and Computational Methods in Nuclear Physics (Springer Lecture Notes in Physics 209)* ed J Dehasa, J Gomez and A Polls (Berlin: Springer) p 1
[14] Wong S S M and French J B 1972 *Nucl. Phys.* A **198** 188
[15] Bohigas O and Giannoni M J 1975 *Ann. Phys., NY* **89** 393
[16] Gurevich I I and Pevsner M I 1956/7 *Nucl. Phys.* **2** 575
[17] Weiss D, Roukes M, Menschig A, Grambow P, von Klitzing K and Weimann G 1991 *Phys. Rev. Lett.* **66** 2790
[18] Graighead H G 1992 *Physics of Nanostructures; Proc. 38th Scottish Universities Summer School in Physics* ed J H Davies and A R Long (Bristol: Institute of Physics Publishing) p 21